Structural Engineering and Mechanics, *Vol. 54, No. 1 (2015) 189-198*
DOI: http://dx.doi.org/10.12989/sem.2015.54.1.189

Torsional analysis of a single-bent leaf flexure

Nghia Huu Nguyen, Byoung-Duk Lim and Dong-Yeon Lee*

School of Mechanical Engineering, Yeungnam University, Gyeongsan 712-749, Republic of Korea

(Received November 12, 2014, Revised January 17, 2015, Accepted February 2, 2015)

Abstract. We present a torsion analysis of single-bent leaf flexure that is partially restrained, subject to a torsional load. The theoretical equations for the torsional angle are derived using Castigliano's theorem. These equations consider the partially restrained warping, and are verified using finite element analysis (FEA). A sensitivity analysis over the length, width, and thickness is performed and verified via FEA. The results show that the errors between the theory result and the FEA result are lower than 6%. This indicates that the proposed theoretical torsional analysis with partially restrained warping is sufficiently accurate.

Keywords: torsion; warping restraint factor; partially restrained warping; leaf flexure; Castigliano's theorem

1. Introduction

A flexure guide has many applications in Micro-Electro-Mechanical Systems (MEMS) and Nano-Electro-Mechanical Systems (NEMS) devices, and plays an important role in nano-scanners. Flexure can generate the smooth motion by the elastic deformations of its body, and is one of the best solutions in applications that require smooth and nano-resolution guiding (Park *et al.* 2010). A flexure is usually designed such that deformation occurs along one or two axes, and deformation is prevented along the other axes (Lobontiu *et al.* 2004). There are several types of flexure guide: hinge flexures, leaf-spring flexures. There have been many studies related to the prediction of the elastic deformations of flexure. For example, an ortho-planar spring design is presented (Parise *et al.* 2001), a flexure guide for a planar positioning mechanism with three degrees of freedom was investigated (Fukada and Nishimura 2007). Flexure with large range and compact dimensions is presented (Yong *et al.* 2009). Hayashi and Fukuda (2012) developed a displacement reduction mechanism based on torsional leaf spring hinges. Formulas have been derived for the stiffness of parallel leaf spring flexure (Brouwer *et al.* 2013). Flexure of plates were investigated by beam theories (Sayyad and Ghugal 2014).

Single leaf flexure is used in many types of motion guides, including simple linear guides, compound linear guides, and double compound linear guides (Brouwer *et al.* 2013). However, the range of travel of single leaf flexure is limited to a very short range (approximately tens of μm) due to the elastic limit. To overcome the short range of travel, a single-bent flexure is examined in this study. In previous studies, torsional analyses for single leaf flexure were considered, and the

*Corresponding author, Professor, E-mail: dylee@ynu.ac.kr

http://www.techno-press.org/?journal=sem&subpage=8 ISSN: 1225-4568 (Print), 1598-6217 (Online)

equations of rotational displacements were derived (Koseki *et al.* 2002, Hayashi and Fukada 2012). However, although the torsion was analysed and calculated in these studies, the warping effect was not sufficiently considered, and one end of the flexure was completely fixed with no partially restrained warping condition. Fully restrained warping over a thin-walled bar was analysed, but the end condition was considered to be completely fixed in (Sapountzakis and Dourakopoulos 2010, Kujawa 2011, Sapountzakis 2012, Yoon *et al.* 2012). The concept of the warping indicator and the partial restraint warping were firstly introduced at the member ends in analyzing space frames (Yang and McGuire 1984). The warping effect was considered and a warping restraint factor was introduced in (Al-HaKeem 1991), and the result was applied to a truck chassis frames.

We performed a torsional analysis of a single-bent leaf flexure with consideration of partially restrained warping and the warping restraint factor (K). The theoretical torsional displacement of the single-bent leaf flexure is derived using Castigliano's second theorem, which considers the strain energy of partially restrained warping over the non-uniform torsion of a homogeneous isotropic prismatic bar. A sensitivity analysis over the length, the width, and the thickness variation is also performed. FEA is used to verify the accuracy of the theoretical analysis. An appropriate warping restraint factor is suggested for the general application of a single leaf flexure in nano-scanner design.

2. Generalized modeling of flexure

Fig. 1 presents the model of the single bent leaf flexure used in this study, which consists of two leaf flexure elements. The dimensions of the structure are length l, width b, and thickness t. In this structure, the flexure acts as a leaf spring. The single leaf spring enables a free end to move smoothly with an appropriate range of travel and no friction. When a torsion T_x is applied at free end of the element 1, then the element 1 twists and the element 2 bends. The joint between element 1 and 2 is not fixed, and is considered to be partially restrained.

Fig. 2 shows an application of the flexure in a planar nano-scanner. The system includes four flexures symmetrically connected to four corners of the square moving body to provide smooth

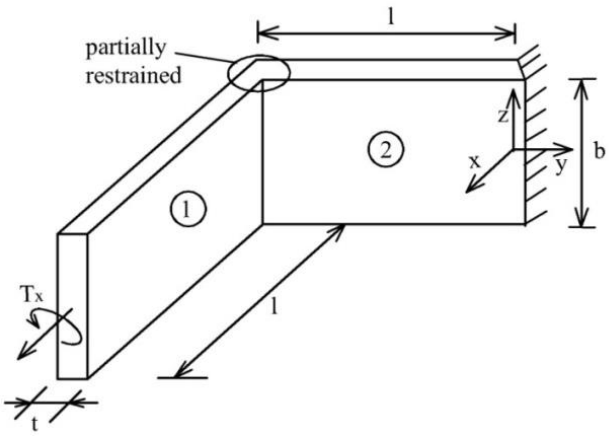

Fig. 1 Schematic diagram of the single bent leaf flexure

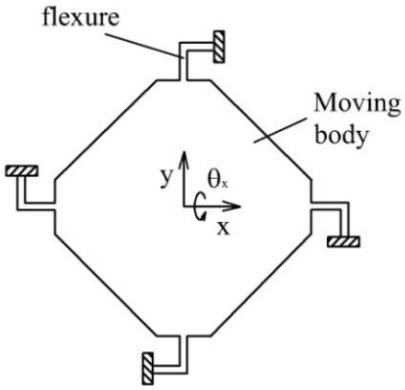

Fig. 2 Schematic diagram of the planar scanner

and non-parasitic error motion. If torsion of the flexure occurs in this system, then out-of-plane motion will occur and the accuracy of the scanner will be low. The present investigation involves analyzing and accurately calculating the rotation when torsion is applied to the flexure.

2.1 Derivation of the total strain energy

In this study, Castigliano's theorem was used to find the rotational displacement of the flexure in Fig. 1. The twist angle was defined by using the partial derivative of the total strain energy with respect to the applied torsion T_x as follows

$$\theta_x = \frac{\partial U}{\partial T_x} \tag{1}$$

where U is the total strain energy that is stored in the flexure and θ_x is the twist angle. When torsion moment T_x is applied to the flexure, it causes torque in element 1 and bending in element 2. Thus, two components of strain energy due to T_x are defined.

2.1.1 Strain energy of torsion in element 1

As previously mentioned, we considered the warping effect when torsion was applied. The governing equation for the non-uniform torsion of a homogeneous isotropic prismatic bar subjected to an end constant torsion T_x is given (Pilkey 2002)

$$GJ_x \frac{d\theta_x}{dx} - EC_w \frac{d^3\theta_x}{dx^3} = T_x \tag{2}$$

where J_x, C_w, G, and E are the torsion constant, warping constant, modulus of transverse elasticity, and modulus of longitudinal elasticity (Young's modulus), respectively. The general solution of Eq. (2) is presented (Pilkey 2002)

$$\theta_x = C_1 + C_2 x + C_3 \cosh\alpha x + C_4 \sinh\alpha x \tag{3}$$

where $\alpha = \sqrt{\frac{GJ_x}{EC_w}}$ is the torsion-bending constant and C_k (k =1, 2, 3, 4) are the constants of integration.

In this studied flexure, the joint between element 1 and 2 was considered to be a flexible joint, which means it was not completely free to warp, but is also not fully restrained. Hence, the joint is partially restrained. Therefore, a warping restraint factor K was introduced to find the degree of partial restraint from warping (Al-HaKeem 1991). The boundary conditions (BCs) of elements 1 and 2 of the flexure were selected as follows. Element 1 was specified to have a partial warping constraint at x=0 and free warping at x=l. BCs were defined in the following two cases:

First case: the complete warping constraint occurs at x=0 and the free constraint occurs at x=l, so the BCs were chosen as follows:

$$\text{At } x = 0,\ \theta_x(0) = 0 \text{ and } \frac{d\theta_x(0)}{dx} = 0$$

$$\text{At } x = l,\ \ M_\omega = 0 \text{ or } \frac{d^2\theta_x}{dx^2} = 0$$

By solving these equations, the constants were determined as follows:

$$C_1 = -\frac{T_x}{\alpha G J_x} tanh\alpha l\ ,\ C_2 = \frac{T_x}{GJ_x}\ ,\ C_3 = \frac{T_x}{\alpha G J_x} tanh\alpha l\ ,\ C_4 = -\frac{T_x}{\alpha G J_x}$$

Therefore, from Eq. (3), the twisting angle is

$$\theta_x = \frac{T_x}{\alpha G J_x}(\alpha x - sinh\alpha x - tanh\alpha l + tanh\alpha l cosh\alpha x) \tag{4}$$

Second case: free warping was considered at both ends (x=0 and x=l) and thus the BCs were selected as follows:

$$\text{At } x{=}0,\ \theta_x(0) = 0 \text{ and } \ M_\omega = 0 \text{ or } \frac{d^2\theta_x}{dx^2} = 0$$

$$\text{At } x{=}l,\ M_\omega = 0 \text{ or } \frac{d^2\theta_x}{dx^2} = 0$$

Similarly, the constants are $C_1 = C_3 = C_4 = 0$, $C_2 = \frac{T_x}{GJ_x}$

Thus, from Eq. (3), the twisting angle is

$$\theta_x = \frac{T_x}{GJ_x} x \tag{5}$$

Then, the warping restraint factor K was introduced into Eqs. (4) and (5), and the rotational displacement of the flexure about the x-axis was defined as follows

$$\theta_x = \frac{T_x}{\alpha G J_x}\left(\alpha x + (1-K)(-sinh\alpha x - tanh\alpha l + tanh\alpha l cosh\alpha x)\right) \tag{6}$$

Eq. (6) shows that when K=0, the fully restrained warping occurred at the end, x=0 (case 1), and free warping occurred when K=1 (case 2). Therefore, first- and second-order derivative equations were determined to be

$$\theta_x^{'} = \frac{d\theta_x}{dx} = \frac{T_x}{GJ_x}\left(1 + (1-K)(-cosh\alpha x + tanh\alpha l sinh\alpha x)\right) \tag{7}$$

$$\text{and } \theta_x^{''} = \frac{d^2\theta_x}{dx^2} = \frac{\alpha T_x}{GJ_x}(1-K)(-sinh\alpha x + tanh\alpha l cosh\alpha x) \tag{8}$$

The torsion constant J_x of the rectangular cross section bar was determined by using Eq. (161) (Timoshenko and Goodier 1951)

$$J_x = \frac{bt^3}{3}\left[1 - 0.63\frac{t}{b}\left(1 - \frac{t^4}{12b^4}\right)\right] \tag{9}$$

The warping constant C_w with respect to the shear center is defined by Eq. (7.43) (Pilkey 2002) as the warping moment of inertia

$$C_w = \int \omega^2 dA = \frac{(bt)^3}{144} \tag{10}$$

where ω is the warping function.

Therefore, the strain energy in element 1 is defined by Eq. (9) (Kujawa 2011)

$$U_1 = \frac{1}{2}EC_w\int_0^l\left(\theta_x^{''}\right)^2 dx + \frac{1}{2}GJ_x\int_0^l\left(\theta_x^{'}\right)^2 dx \tag{11}$$

2.1.2 Strain energy of bending in element 2

T_x causes the bending in element 2 of flexure, thus the strain energy of bending was defined as follows

$$U_2 = \int_0^l \frac{(T_x)^2}{2EI_x} dy \tag{12}$$

Where $I_x = \frac{tb^3}{12}$ is the moment of inertia about the x-axis. From Eqs. (11) and (12), the total strain energy was determined as follows

$$U = U_1 + U_2 = \frac{1}{2}EC_w\int_0^l\left(\theta_x^{''}\right)^2 dx + \frac{1}{2}GJ_x\int_0^l\left(\theta_x^{'}\right)^2 dx + \int_0^l \frac{(T_x)^2}{2EI_x} dy \tag{13}$$

2.2 Twist angle

Integrating Eq. (13) yields

$$U = \frac{\alpha EC_w T_x^2\left(K^2 sinh\alpha l - sinh\alpha l + \alpha l cosh\alpha l\right)}{2G^2 J_x^2 cosh\alpha l} + \frac{(T_x)^2}{2EI_x} \tag{14}$$

Therefore, from Eq. (14), the twist angle at the free end of the single bent flexure under torsion load T_x is defined as follows

$$\theta_x = \frac{\partial U}{\partial T_x} = \frac{\alpha EC_w T_x\left(K^2 sinh\alpha l - sinh\alpha l + \alpha l cosh\alpha l\right)}{G^2 J_x^2 cosh\alpha l} + \frac{T_x l}{EI_x} \tag{15}$$

3. FEA Verification

FEA was conducted by using Pro-Mechanica commercial software (Wildfire 5, PTC Corp., MA, USA) to verify the results of theoretical method. The default values of the flexure are as follows: length l=10 mm, width b=4 mm, and thickness t=0.5 mm. The torsion moment is T_x=1 N mm. The material used in this simulation is aluminum 6061. We performed a parametric analysis wherein the sensitive parameters were used to check the agreement between the FEA results and theory results, with the following variations: length l=5 to 20 mm, width b=2 to 8 mm, and thickness t =0.25 to 1 mm. Fig. 3 shows the FEA model with the 48 elements and 36 nodes.

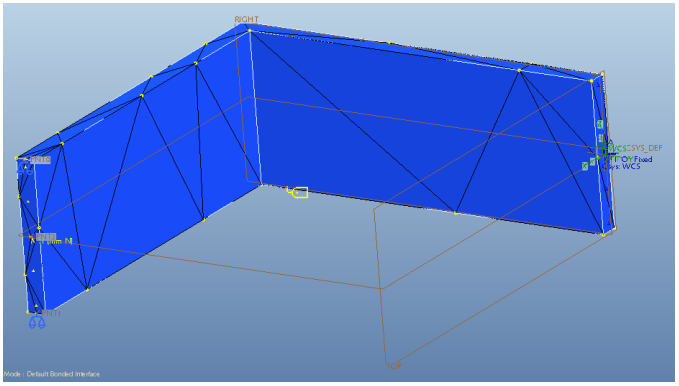

Fig. 3 FEA model

Table 1 Comparison between theory and FEA results at the default values of flexure

	Method	Rotational displacement, θ_x (mrad)	Error between FEA and theory (%)
	FEA	2.39	-
Theory	Fully restrained warping (K=0)	2.27	4.7
	Partially restrained warping (K=0.5)	2.33	2.2
	Free warping (K=1)	2.51	-5.3

Our goal in this study was to find the displacement of the flexure when the torsion moment is applied at the free end of the single bent flexure and then compare these results with the results from FEA. If the error between the two methods was lower than 10%, then the results were generally accepted and used in the subsequent design steps.

3.1 Comparison at default values

Eq. (15) was used to find the theoretical rotational displacements. The warping restraint factor K values were K=0, 0.5, and 1. The FEA simulation was also conducted at the default values of flexure. Table 1 shows a comparison between the theoretical and FEA results. As shown in Table 1, the error for K=0.5 was the lowest at 2.2%, and the errors for K=0 and K=1 were 4.7% and 5.3%, respectively. Thus, when the appropriate partial restraint factor were considered in the analysis, the result of rotation under torsion T_x is quite close to the FEA result. The joint between element 1 and element 2 of the flexure was not fully fixed and also not fully free. This indicates that derived rotational equation based on theory with K=0.5 is in good agreement with the FEA results, and that these results could be accepted for use in the subsequent investigations.

3.2 Sensitive parameter analysis

Fig. 4 shows the results obtained using theory and FEA to simulate the variation of rotation θ_x for length l=5 to 20 mm under torsion T_x. We note that when length l increases, the rotation θ_x increases linearly using both methods. Fig. 4 shows that the theory results are in good agreement with the FEA results: the errors are 6% lower (K=0.5) as shown in Table 2.

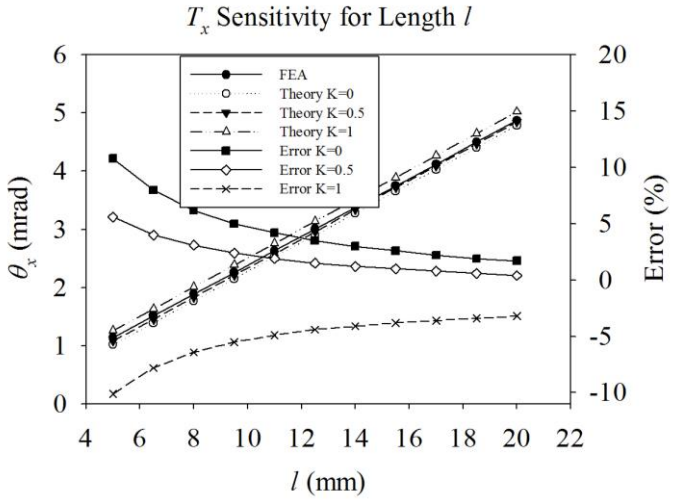

Fig. 4 Variation of θ_x according to length l under torsion T_x

Table 2 Rotation θ_x (mrad) from theory and FEA according to length l under torsion T_x

Length (mm)	FEA	Theory			Error (%)		
		K=0	K=0.5	K=1	K=0	K=0.5	K=1
5	1.14	1.02	1.08	1.26	10.8	5.6	-10.1
6.5	1.52	1.39	1.45	1.63	8.0	4.0	-7.8
8	1.89	1.77	1.83	2.01	6.2	3.1	-6.4
9.5	2.26	2.15	2.21	2.39	5.0	2.4	-5.5
11	2.63	2.53	2.58	2.76	4.2	1.9	-4.9
12.5	3.01	2.90	2.96	3.14	3.5	1.5	-4.4
14	3.38	3.28	3.34	3.52	3.0	1.2	-4.1
15.5	3.75	3.66	3.72	3.89	2.6	1.0	-3.8
17	4.12	4.03	4.09	4.27	2.2	0.8	-3.6
18.5	4.50	4.41	4.47	4.65	1.9	0.6	-3.4
20	4.87	4.79	4.85	5.02	1.7	0.4	-3.2

Fig. 5 shows the results of the variation of rotation θ_x according to the thickness t=0.25 to 1 mm under torsion T_x based on theory and FEA. When the thickness t increases, the rotation θ_x decreases in both methods. These graphs show that the theory results are in good agreement with FEA results: the errors were 4% lower (K=0.5) as shown in Table 3. Similarly, Fig. 6 shows the results of the variation of rotation θ_x according to the width b=2 to 8 mm under torsion T_x based on theory and FEA. When the width b increases, the rotation θ_x is smaller in both methods. These graphs show that results of theory are in strong agreement with the results of FEA: the errors are 5% lower (K=0.5) as shown in Table 4.

The warping and partially restrained effects (K=0.5) were considered in the analysis. The results are compared with fixed (no warping, K=0) and free (free warping, K=1) boundary conditions at the joint between two elements of the flexure, as shown in Figs. 3-5 and Tables 2-4.

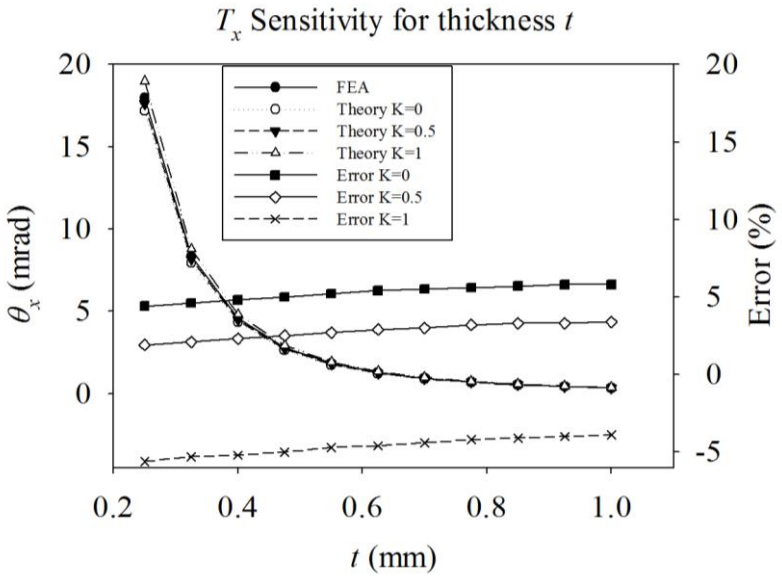

Fig. 5 Variation of θ_x according to thickness t under torsion T_x

Table 3 Rotation θ_x (mrad) results for theory and FEA according to thickness t under torsion T_x

Thickness (mm)	FEA	Theory			Error (%)		
		K=0	K=0.5	K=1	K=0	K=0.5	K=1
0.25	17.95	17.17	17.62	18.96	4.4	1.9	-5.6
0.325	8.33	7.94	8.15	8.77	4.6	2.1	-5.3
0.4	4.55	4.33	4.45	4.79	4.8	2.3	-5.2
0.475	2.77	2.64	2.70	2.91	5.0	2.5	-5.0
0.55	1.83	1.73	1.78	1.91	5.2	2.7	-4.7
0.625	1.27	1.20	1.23	1.33	5.4	2.9	-4.6
0.7	0.93	0.87	0.90	0.97	5.5	3.0	-4.4
0.775	0.70	0.66	0.68	0.73	5.6	3.2	-4.2
0.85	0.54	0.51	0.52	0.56	5.7	3.3	-4.1
0.925	0.43	0.41	0.42	0.45	5.8	3.3	-4.0
1	0.35	0.33	0.34	0.36	5.8	3.4	-3.9

The error is 4.7% if fixed, 5.3% if free, and 2.2% if partially restrained at the default values. The errors in the free warping sensitivity analysis are up to 12%. The fully restrained warping (fixed) error is 11% and the partially restrained error is lower than 6%. These results indicate that the error in the rotational displacement of flexure under torsion changed with variations of the length, thickness, width and the warping restraint factor. However, the results obtained using theory and FEA at K=0.5 are quite similar: the errors were lower than 6% in all the simulated analyses. Thus, there is strong agreement between the two methods, which demonstrates the validity of the theoretical equations for the case under consideration.

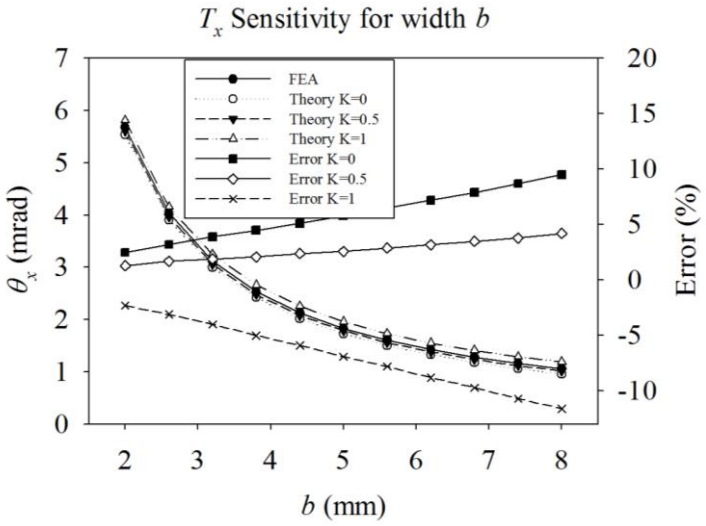

Fig. 6 Variation of θ_x according to width b under torsion T_x.

Table 4 Rotation θ_x (mrad) of theory and FEA according to width b under torsion T_x

Width (mm)	FEA	Theory			Error (%)		
		K=0	K=0.5	K=1	K=0	K=0.5	K=1
2	5.68	5.54	5.61	5.81	2.5	1.3	-2.3
2.6	4.04	3.91	3.97	4.16	3.2	1.7	-3.1
3.2	3.12	3.00	3.06	3.25	3.9	1.9	-4.0
3.8	2.54	2.42	2.48	2.66	4.5	2.1	-5.0
4.4	2.13	2.02	2.08	2.26	5.1	2.4	-5.9
5	1.83	1.73	1.79	1.96	5.8	2.6	-6.9
5.6	1.61	1.50	1.56	1.73	6.5	2.9	-7.8
6.2	1.43	1.33	1.38	1.55	7.2	3.2	-8.8
6.8	1.28	1.18	1.24	1.41	7.9	3.5	-9.7
7.4	1.16	1.06	1.12	1.29	8.7	3.8	-10.7
8	1.06	0.96	1.02	1.19	9.5	4.2	-11.6

4. Conclusions

In this study, the torsion of a single bent leaf flexure with consideration of partially-restrained warping and the warping restraint factor (K) were analyzed. The equations of rotation displacement under torsion of the flexure were developed based on Castigliano's theorem, which considers the strain energy of partially restrained warping over the non-uniform torsion of a homogeneous isotropic prismatic bar. A sensitivity analysis with respect to the length, width, and thickness variation was performed, and FEA was conducted to verify the accuracy of the theoretical analysis. These results reveals the accuracy of the present analysis and could be used in the design of the nano-system.

Acknowledgments

This research was supported by Basic Science Research Program through the National Research Foundation of Korea (NRF) funded by the Ministry of Education (NRF-2013R1A1A4A01009657).

References

Brouwer, D.M., Meijaard, J.P. and Jonker, J.B. (2013), "Large deflection stiffness analysis of parallel prismatic leaf-spring flexures", *J. Precis. Eng.*, **37**(3), 505 - 521.

Fukada, S. and Nishimura, K. (2007), "Nanometric positioning over a one-millimeter stroke using a flexure guide and electromagnetic linear motor", *Int. J. Precis. Eng. Man*., **8**(2), 49-53.

Hayashi, M. and Fukuda, M. (2012), "Generation of Nanometer Displacement using Reduction Mechanism Consisting of Torsional Leaf Spring Hinges", *Int. J. Precis. Eng. Man.*, **13**(5), 679-684.

Koseki, T.T.Y., Arai, T. and Koyachi, N. (2002), "Kinematic Analysis of Translational 3-DOF Micro Parallel Mechanism Using Matrix Method", *Adv. Robot.*, **16**(3), 251-264.

Kujawa, M. (2011), "Torsion of restrained thin-walled bars of open constraint bisymmetric cross-section", *Tast quarterly*, **16**(1), 5-15.

Lobontiu, N., Garcia, E. and Canfield, S. (2004), "Torsional stiffness of several variable rectangular cross-section flexure hinges for macro-scale and MEMS applications", *Smart Mater. Struct*., **13**(1), 12-19.

Parise J.J., Howell, L.L. and Magleby, S.P. (2001), "Ortho-planar linear-motion springs", *Mech. Mach. Theory*, **36**(11), 1281-1299.

Park, E.J., Shim, J., Lee, D.Y. and Lee, J. (2010), "A double-bent planar leaf flexure guide for a nano-scanner", *J. Korean Phys. Soc*., **57**(6), 1581-1588.

Sapountzakis, E.J. (2012), "Bars under torsional loading: a generalized beam theory approach", *ISRN Civil Eng.*, 1-39.

Sapountzakis, E.J. and Dourakopoulos, J.A. (2010), "Shear deformation effect in flexural-torsional buckling analysis of beams of arbitrary cross section by BEM", *Struct. Eng. Mech.*, **35**(2), 141-173.

Sayyad, A.S. and Ghugal, Y.M. (2014), "Flexure of cross-ply laminated plates using equivalent single layer trigonometric shear deformation theory", *Struct. Eng. Mech.*, **51**(5), 867-891.

Yong, Y.K., Aphale, S.S. and Moheimani, S.O.R. (2009), "Design, Identification, and Control of a Flexure-Based XY Stage for Fast Nanoscale Positioning", *IEEE T. Nanotechnol*., **8**(1), 46-54.

Yoon, K., Lee, Y. and Lee, P.S. (2012), "A continuum mechanics based 3-D beam finite element with warping displacements and its modeling capabilities", *Struct. Eng. Mech.*, **43**(4), 411-437.

Pilkey, W.D. (2002), *Analysis and design of elastic beams: computational methods*, John Wiley & Sons Inc. New York, USA.

Timoshenko, S.P. and Goodier, J.N. (1951), *Theory of Elasticity,* McGraw-Hill Book Company, New York, USA.

Yang, Y.B. and McGuire, W. (1984), "A procedure for analysing space frames with partial warping restraint", *Int. J. Numer. Meth. Eng.*, **20**, 1377-1398.

Al-HaKeem, A.H. (1991), "Structural analysis of truck chassis frames under longitudinal loads considering bimoment effects", Ph.D. Dissertation, Cranfield Institute of Technology, Cranfield.

PL